

## Molecular Electronics

**Electron Transfer in a Hg-SAM//SAM-Hg Junction Mediated by Redox Centers\*\***

Elizabeth Tran, Maria A. Rampi,\* and George M. Whitesides\*

Studies of electron transport through molecules using metal–molecule–metal junctions<sup>[1–3]</sup> or scanning probe devices<sup>[2,4–6]</sup> suggest principles that may be useful in designing systems for organic/organometallic electronics. Molecules are, in general, poor conductors of electrons, and “conduct” by tunneling. For some molecules, however, applying a potential across the electrodes of a metal–molecule–metal junction can cause an orbital (usually the HOMO or LUMO) of the molecule to fall between the Fermi levels of the electrodes and thus increase conductivity.<sup>[7,8]</sup> Molecules with well-defined and readily accessible redox states are, thus, attractive candidates for use in testing theories of electron transport (and perhaps for electronic devices),<sup>[4,9–18]</sup> and a few examples are now known in which two or more metal redox centers organized in space and energy with respect to one another display electronic functions such as rectification and switching.<sup>[19,20]</sup> Here we report the first example of a metal–molecule–metal junction comprising two closely spaced alkane thiolate monolayers,

[\*] Prof. M. A. Rampi

Dipartimento di Chimica, Università di Ferrara  
via L. Borsari 46, 44100 Ferrara (Italy)  
Fax: (+39) 053-229-1162  
E-mail: rmp@unife.it

Dr. E. Tran, Prof. G. M. Whitesides  
Department of Chemistry and Chemical Biology  
Harvard University, Cambridge, MA 02138 (USA)  
Fax: (+1) 617-495-9857  
E-mail: gwhitesides@gmwgroup.harvard.edu

[\*\*] The support of DARPA, NSEC (award no. NSF-PHY-0117795), EC (award no. G5RD-CT-2002-00776 MWFM), and NSERC (in the form of a postdoctoral fellowship to E.T.) is gratefully acknowledged. We thank Prof. Royce Murray, Prof. Wolfgang Schmickler, Mandar Deshmukh, Mark Gudiksen, Amy Prieto, Babak Parviz, Logan McCarty, Rosaria Ferrigno, and Sam Sia for helpful discussions, and Prof. Harry Finklea for providing a procedure for the synthesis of the ruthenium-containing thiol.



Supporting information for this article is available on the WWW under <http://www.angewandte.org> or from the author.

each presenting redox centers at their surface.<sup>[21]</sup> Standard electrochemical techniques demonstrate that this junction becomes conductive when the electrode potentials are adjusted to the formal potential of the redox centers, and that it shows diode- and transistor-like characteristics analogous to those of solid-state devices.

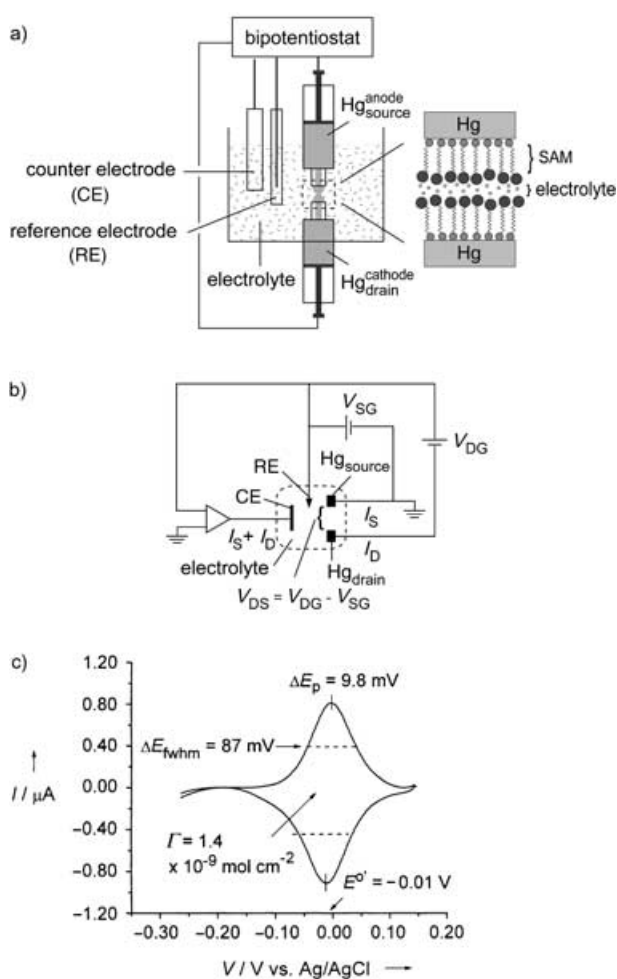
Figure 1a shows a schematic illustration of the junction<sup>[22–30]</sup> and the associated electrochemical system. The junction consists of two mercury-drop electrodes, both of which support a self-assembled monolayer (SAM) of the thiol terminated with the ruthenium pentamine pyridine-terminated thiol [Ru(NH<sub>3</sub>)<sub>5</sub>(NC<sub>5</sub>H<sub>4</sub>-4-CH<sub>2</sub>NHCO(CH<sub>2</sub>)<sub>10</sub>SH)(PF<sub>6</sub>)<sub>2</sub>] (henceforth abbreviated as HS-C<sub>10</sub>-Ru).<sup>[31,32]</sup> The thiol HS-C<sub>10</sub>-Ru readily adsorbs from 1 mM acetonitrile solutions onto mercury electrodes and gives electroactive monolayers.<sup>[33]</sup> Cyclic voltammetry of a mono-

layer in contact with 0.2 M aqueous Na<sub>2</sub>SO<sub>4</sub> at pH 4 (Figure 1c) shows a redox wave corresponding to the Ru<sup>II</sup>↔Ru<sup>III</sup> interconversion at  $E_{\text{SAM}}^{\text{of}} = -0.01$  V versus Ag/AgCl, a value that is close to that of a related compound dissolved in the same medium ( $E_{\text{soln}}^{\text{of}} = +0.04$  V versus the saturated calomel electrode<sup>[31]</sup>). At scan rates < 100 mV s<sup>-1</sup>, the oxidation and reduction peaks are stable to electrochemical cycling over at least 16 scans, and essentially symmetric, with a peak separation of < 10 mV and a full-width at half-maximum of about 90 mV. This ideal behavior indicates that the ruthenium moieties are uniform in their redox behavior. We infer that these moieties are located at the external surface of the monolayer.

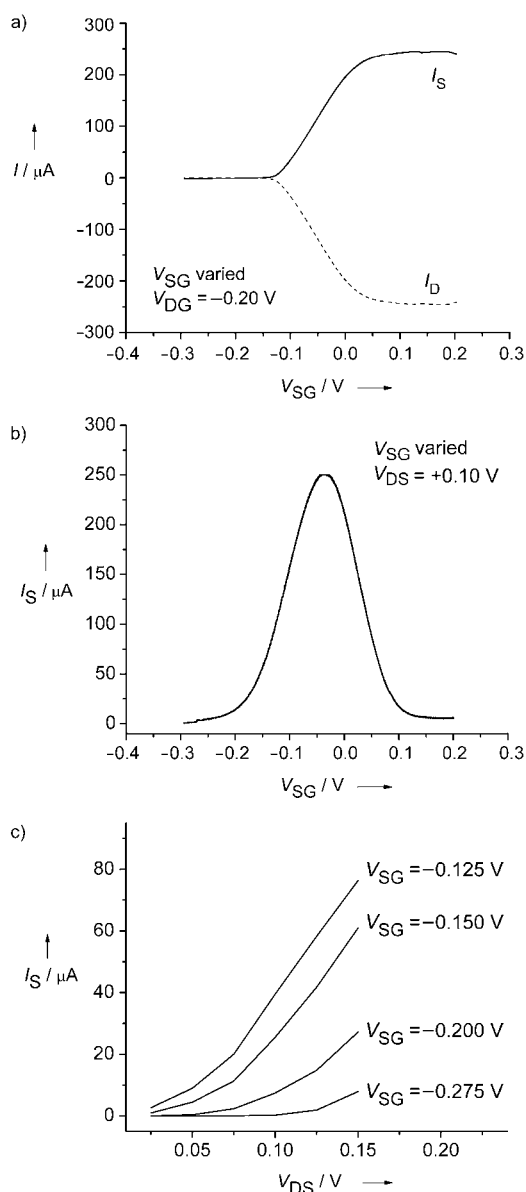
We studied electron transport across the Hg-SAM//SAM-Hg junction by placing the junction, together with an Ag/AgCl reference electrode and a platinum counter electrode, in a Na<sub>2</sub>SO<sub>4</sub> electrolyte solution at pH 4, and by using a bipotentiostat that allowed the potentials of the mercury electrodes to be controlled independently with respect to the reference electrode (Figure 1a). The potentials of the mercury electrodes were controlled such that one (cathode) acted as an electron donor and the other (anode) as an electron acceptor. We designated the cathode and anode as the drain and source electrodes, respectively, by analogy to the convention used in semiconductor devices, where current is considered to flow from a more positive region to a more negative region.<sup>[34]</sup> We measured the conductance through the junction as a function of the potentials of the drain and source electrodes with respect to the reference electrode (that is,  $V_{\text{DG}}$  and  $V_{\text{SG}}$ , respectively) and as a function of the potential between the source and drain ( $V_{\text{DS}}$ ) using the electrolyte solution as a gate.<sup>[35]</sup> We controlled the potential of the gate by controlling the potential applied to the reference electrode relative to the ground potential. Since the source electrode is at ground potential, this voltage is  $V_{\text{SG}}$ .

Figure 2a shows the drain/source currents when  $V_{\text{DG}}$  is fixed at -0.20 V, whereby the attached ruthenium is in its +2 oxidation state, and  $V_{\text{SG}}$  is varied. The currents are negligible and the junction is nonconducting for  $V_{\text{SG}} \leq V_{\text{DG}}$ . Increasing  $V_{\text{SG}}$  to values more positive than -0.14 V results in an anodic current flow corresponding to the oxidation of Ru<sup>II</sup> to Ru<sup>III</sup> at the source and a cathodic current flow corresponding to the reduction of Ru<sup>III</sup> to Ru<sup>II</sup> at the drain. The anodic and cathodic currents are equal and increase to a plateau with a half-wave (half-maximum) potential (-0.04 V) that is near the formal potential  $E^{\text{of}}$  of the Ru<sup>II</sup>/Ru<sup>III</sup> couple. The maximum current passing through the electrodes with an electrode contact area of about 0.20 mm<sup>2</sup> is typically about 1.3 mA mm<sup>-2</sup> (or 1000 electrons per second per molecule), a value that is approximately 600-fold higher than that observed when only one of the mercury electrodes is electrically connected to the bipotentiostat.

The observation that the current depends on the  $E^{\text{of}}$  value of the redox couple is evidence that charge transport in the junction is related to the presence of the surface-bound redox centers. To determine whether charge transport requires redox centers on both electrodes, we replaced the drain electrode with a bare mercury electrode in one experiment and with a mercury electrode modified with the non-electro-



**Figure 1.** Schematic representations of a) the Hg-SAM//SAM-Hg junction and the electrochemical system used to characterize it, and b) the electrical circuit for the experimental setup in (a).  $V_{\text{SG}}$  and  $V_{\text{DG}}$  are the potentials of the source and drain electrodes with respect to the reference electrode, respectively. The electrolyte is the gate whose potential is established by the voltage applied to the reference electrode relative to ground.  $I_{\text{D}}$  and  $I_{\text{S}}$  are the currents at the drain and source electrodes. c) Cyclic voltammogram (corrected for charging current) for a mercury-drop electrode supporting a SAM of HS-C<sub>10</sub>-Ru in contact with 0.2 M aqueous Na<sub>2</sub>SO<sub>4</sub> at pH 4. The scan rate was 50 mV s<sup>-1</sup>.



**Figure 2.** Current–voltage characteristics of the Hg-SAM//SAM-Hg junction showing diodelike and transistor-like behavior. All experiments were carried out in 0.2 M aqueous  $\text{Na}_2\text{SO}_4$  at pH 4. a)  $I_D$  and  $I_S$  as a function of  $V_{SG}$ .  $V_{DG}$  was fixed at  $-0.20$  V and the scan rate was  $50 \text{ mVs}^{-1}$ . b)  $I_S$  as a function of  $V_{SG}$  for the same junction as in (a).  $V_{DS}$  was fixed at  $+0.10$  V. c)  $I_S$  as a function of  $V_{DS}$  at different values of  $V_{SG}$ . For (b) and (c),  $I_D$  (not shown) is equal in magnitude but opposite in sign to  $I_S$ ; the scan rate was  $10 \text{ mVs}^{-1}$ .

active thiol  $\text{HS}(\text{CH}_2)_{10}\text{COOH}$  in another. In both experiments, we observed negligible current at the drain and a peak-shaped voltammetric wave consistent with reversible oxidation of  $\text{Ru}^{\text{II}}$  to  $\text{Ru}^{\text{III}}$  at the source. The current level at the source was in the range ( $< 10\%$  difference) of that observed in the cyclic voltammogram and suggested that electron transfer between an electrode and its redox-active SAM is faster than electron transfer between an electrode and the redox centers on the neighboring electrode. The presence of redox centers on both electrodes is therefore needed for current to pass from one electrode to another.

Based on these observations, we propose that charge transport through the junction occurs as a result of oxidation of  $\text{Ru}^{\text{II}}$  to  $\text{Ru}^{\text{III}}$  at the source, electron exchange between  $\text{Ru}^{\text{III}}$  at the source and  $\text{Ru}^{\text{II}}$  at the drain, and reduction of  $\text{Ru}^{\text{III}}$  at the drain back to  $\text{Ru}^{\text{II}}$  as key steps (Figure 3).<sup>[36]</sup> Similar

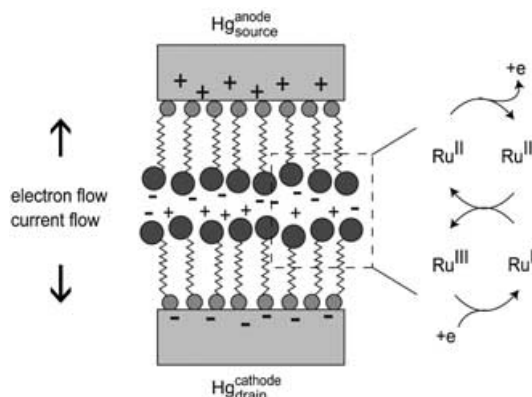


**Figure 3.** Schematic diagram of the proposed mechanism of charge transport through the Hg-SAM//SAM-Hg junction when  $V_{SG}$  is more positive than  $-0.14$  V and  $V_{DG} = -0.14$  V.

surface-to-surface charge-transport mechanisms have been reported previously for a variety of interfaces including polymer/polymer<sup>[37,38]</sup> and polymer/electrolyte solutions;<sup>[39]</sup> such electron-transport processes, however, have not been reported for molecular monolayers. The work reported here thus shows that the magnitude of current flow can be controlled by controlling the potential of the two electrodes with respect to the  $E^{\circ}$  value of the redox couple. Significantly, the current can be made to flow unidirectionally, in a diodelike sense, depending on the applied potential.

The conductance of the Hg-SAM//SAM-Hg junction operating at fixed drain-source potentials is shown in Figure 2b and c. Figure 2b shows that at a fixed  $V_{DS}$  value of  $+0.10$  V, the source current is negligible for a  $V_{SG}$  value of less than  $-0.25$  V and greater than  $+0.15$  V. Scanning  $V_{SG}$  from  $-0.25$  to  $+0.15$  V results in the current increasing from zero to a maximum near the  $E^{\circ}$  value of the redox couple and then decreasing again to zero. Charge therefore passes from one electrode to another only when the value of  $V_{SG}$  is at or close to the  $\text{Ru}^{\text{II}}/\text{Ru}^{\text{III}}$  redox potential. Figure 2c shows that when the  $V_{SG}$  value is below the threshold value required for the oxidation of  $\text{Ru}^{\text{II}}$  to  $\text{Ru}^{\text{III}}$  to occur, the source current is essentially zero at all values of  $V_{DS}$ . Upon changing  $V_{SG}$  to potentials more positive than the threshold value, the current increases with increasing  $V_{DS}$  as  $V_{SG}$  approaches  $E^{\circ}$ . The observation that the current scales with  $V_{SG}$  (the gate potential) is indicative of transistor-like behavior. Unlike conventional solid-state devices which exhibit linear and saturation regions for a given applied gate bias, however, the current passing through the Hg-SAM//SAM-Hg junction described here increases nonlinearly with increasing  $V_{DS}$  values. Similar current–potential curves have been reported for a number of systems,<sup>[40,41]</sup> where charge transport has also been proposed to occur by an electron hopping mechanism. Such

behavior has been attributed to field-dependent charge mobility.

The observation that current passing from one electrode to another depends on the values of both  $V_{SG}$  and  $V_{DS}$  can also be explained in terms of an energy diagram relating the potential of the mercury electrodes on the Ag/AgCl scale to a vacuum and to the corresponding Fermi energy. The potential of the mercury electrodes with respect to Ag/AgCl is related to the absolute potential ( $V_{\text{vacuum}}$ ) and the Fermi energy ( $U_F$ ) by the equations:  $V_{\text{vacuum}} = V_{\text{Ag/AgCl}} + 4.63 \text{ V}$  and  $U_F = -4.63 \text{ eV} - eV_{\text{Ag/AgCl}}$ , respectively.<sup>[42]</sup> Figure 4 indicates that

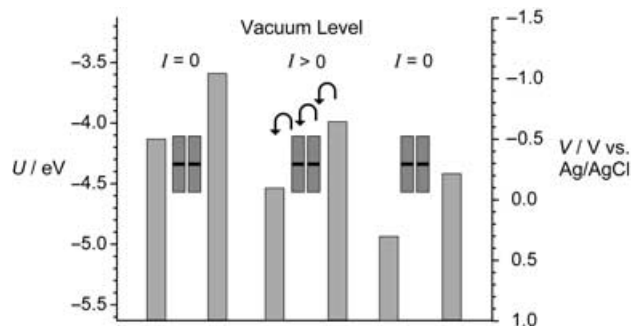


**Figure 4.** Relationship between the electrochemical potential of the Ru<sup>II</sup>/Ru<sup>III</sup> couple measured on the Ag/AgCl scale and the position of the Fermi energy of the mercury electrodes. More negative potentials on the Ag/AgCl scale are closer to vacuum. The small boxes represent the potential limits for the Ru<sup>II</sup> ↔ Ru<sup>III</sup> interconversion.

when both the drain and source electrodes are at potentials very negative or very positive relative to  $E^0$ , no current flows and the junction is nonconducting. The only time the current flows is when the electronic states of the Ru<sup>II</sup>/Ru<sup>III</sup> couple fall between the Fermi energies of the source and the drain. This situation can be achieved by changing the value of  $V_{DS}$  and/or  $V_{SG}$ .

In conclusion, a system based on a Hg-SAM//SAM-Hg junction is described that allows the incorporation of two monolayers of redox-active centers between the mercury electrodes and the potentials of the two mercury electrodes to be controlled independently with respect to the formal potential of the redox centers. In this system, electron transport through the molecules can be controlled readily by tuning the Fermi energy of the mercury electrodes relative to the energy of the redox centers; this potential control not only determines the direction but also the magnitude of current flow through the junction. The junction switches from *off* to *on* when the electronic states of the redox centers on the two monolayers fall between the Fermi levels of the electrodes. Only when the junction has Ru<sup>II</sup>/Ru<sup>III</sup> centers on both electrodes does it conduct electrons (under appropriate conditions); this conduction depends on the number of redox centers trapped in the area in which the two compliant mercury electrodes are in contact, and on the rates of a) electron tunneling between the mercury electrodes and the surface-bound Ru<sup>II</sup>/Ru<sup>III</sup> centers and b) electron hopping between adjacent Ru<sup>II</sup> and Ru<sup>III</sup> centers.

The junction shows electrical behavior similar to that of a solid-state transistor when the electrolyte is used as the gate. The channel length in this case is defined essentially by the

thickness of the SAMs between the two mercury electrodes. Although the system is mechanically less stable than conventional field-effect transistors (FETs) and is limited in value for studying the influence of temperature on electron-transfer rates (because of the liquid mercury electrodes), the system described here is easy to assemble and makes it easy to modify both the area and electrical properties of the metal–metal junction. The area can be modified by changing the pressure applied to the mercury electrodes, while tuning of the electrical properties may be achieved by changing the nature of the redox centers, and the length and structure of the hydrocarbon chains anchoring these centers. Finally, the junction is well-characterized and yields reproducible data, and thus it is well-suited for collecting fundamental information relevant to the fabrication of molecular switches and field-effect transistors.

Received: February 5, 2004 [Z53945]

**Keywords:** electron transfer · mercury · molecular electronics · monolayers · redox chemistry

- [1] W. Wang, T. Lee, M. A. Reed, *Phys. Rev. B* **2003**, *68*, 035416.
- [2] L. A. Bumm, J. J. Arnold, M. T. Cygan, T. D. Dunbar, T. P. Burgin, L. Jones II, D. L. Allara, J. M. Tour, P. S. Weiss, *Science* **1996**, *271*, 1705.
- [3] J. G. Kushmerick, D. B. Holt, J. C. Yang, J. Naciri, M. H. Moore, R. Shashidhar, *Phys. Rev. Lett.* **2002**, *89*, 086802.
- [4] W. Han, E. N. Durantini, A. L. Moore, D. Gust, P. Rez, G. Leatherman, G. R. Sealey, N. J. Tao, S. M. Lindsay, *J. Phys. Chem. B* **1997**, *101*, 10719.
- [5] Z. J. Donhauser, B. A. Mantooth, K. F. Kelly, L. A. Bumm, J. D. Monnell, J. J. Stapleton, D. W. Price, Jr., A. M. Rawlett, D. L. Allara, J. M. Tour, P. S. Weiss, *Science* **2001**, *292*, 2303.
- [6] X. D. Cui, A. Primak, X. Zarate, J. Tomfohr, O. F. Sankey, A. L. Moore, T. A. Moore, D. Gust, G. Harris, S. M. Lindsay, *Science* **2001**, *294*, 571.
- [7] A. Nitzan, M. A. Ratner, *Science* **2003**, *300*, 1384.
- [8] D. Cahen, G. Hodes, *Adv. Mater.* **2002**, *14*, 789.
- [9] D. I. Gittins, D. Bethell, D. J. Schiffrin, R. J. Nichols, *Nature* **2000**, *408*, 67.
- [10] J. Park, A. N. Pasupathy, J. I. Goldsmith, C. Chang, Y. Yaish, J. R. Petta, M. Rinkoski, J. P. Sethna, H. D. Abruna, P. L. McEuen, D. C. Ralph, *Nature* **2002**, *417*, 722.
- [11] W. Liang, M. P. Shores, M. Bockrath, J. R. Long, H. Park, *Nature* **2002**, *417*, 725.
- [12] J. Chen, M. A. Reed, A. M. Rawlett, J. M. Tour, *Science* **1999**, *286*, 1550.
- [13] N. J. Tao, *Phys. Rev. Lett.* **1996**, *76*, 4066.
- [14] D. L. Feldheim, C. D. Keating, *Chem. Soc. Rev.* **1998**, *27*, 1.
- [15] U. Mazur, K. W. Hipps, *J. Phys. Chem. B* **1999**, *103*, 9721.
- [16] R. A. Wassel, G. M. Credo, R. R. Fuierer, D. L. Feldheim, C. B. Gorman, *J. Am. Chem. Soc.* **2004**, *126*, 295.
- [17] W. Haiss, H. van Zalinge, S. J. Higgins, D. Bethell, H. Höbenreich, D. J. Schiffrin, R. J. Nichols, *J. Am. Chem. Soc.* **2003**, *125*, 15294.
- [18] R. Rinaldi, A. Biasco, G. Maruccio, R. Cingolani, D. Alliata, L. Andolfi, P. Facci, F. De Rienzo, R. Di Felice, E. Molinari, *Adv. Mater.* **2002**, *14*, 1449.
- [19] C. Patoux, C. Coudret, J.-P. Launay, C. Joachim, A. Gourdon, *Inorg. Chem.* **1997**, *36*, 5037.
- [20] R. M. Metzger, B. Chen, U. Hopfner, M. V. Lakshminantham, D. Vuillaume, T. Kawai, X. Wu, H. Tachibana, T. V. Hughes, H.

- Sakurai, J. W. Baldwin, C. Hosch, M. P. Cava, L. Brehmer, G. J. Ashwell, *J. Am. Chem. Soc.* **1997**, *119*, 10455.
- [21] For analysis of the electron transport properties of this system, see W. Schmickler, M. A. Rampi, E. Tran, G. M. Whitesides, *Faraday Discuss.* **2004**, *125*, 171.
- [22] K. Slowinski, H. K. Y. Fong, M. Majda, *J. Am. Chem. Soc.* **1999**, *121*, 7257.
- [23] R. E. Holmlin, R. Haag, M. L. Chabinyc, R. F. Ismagilov, A. E. Cohen, A. Terfort, M. A. Rampi, G. M. Whitesides, *J. Am. Chem. Soc.* **2001**, *123*, 5075.
- [24] R. E. Holmlin, R. F. Ismagilov, R. Haag, V. Mujica, M. A. Ratner, M. A. Rampi, G. M. Whitesides, *Angew. Chem.* **2001**, *113*, 2378; *Angew. Chem. Int. Ed.* **2001**, *40*, 2316.
- [25] R. L. Young, P. T. Nguyen, K. Slowinski, *J. Am. Chem. Soc.* **2003**, *125*, 5948.
- [26] Y. Selzer, A. Salomon, D. Cahen, *J. Phys. Chem. B* **2002**, *106*, 10432.
- [27] Y. Selzer, A. Salomon, D. Cahen, *J. Am. Chem. Soc.* **2002**, *124*, 2886.
- [28] R. Haag, M. A. Rampi, R. E. Holmlin, G. M. Whitesides, *J. Am. Chem. Soc.* **1999**, *121*, 7895.
- [29] R. L. York, P. T. Nguyen, K. Slowinski, *J. Am. Chem. Soc.* **2003**, *125*, 5948.
- [30] H.-Z. Yu, Y.-J. Liu, *ChemPhysChem* **2003**, *4*, 335.
- [31] H. O. Finklea, D. D. Hanshew, *J. Am. Chem. Soc.* **1992**, *114*, 3173.
- [32] H. O. Finklea, D. D. Hanshew, *J. Electroanal. Chem.* **1993**, *347*, 327.
- [33] The Supporting Information provided with this paper includes details of the experimental protocols and a cyclic voltammogram (uncorrected for charging current) of a mercury electrode coated with a monolayer of  $[\text{Ru}(\text{NH}_3)_5(\text{NC}_3\text{H}_4-4\text{-CH}_2\text{NHCO}(\text{CH}_2)_{10}\text{SH})(\text{PF}_6)_2$
- [34] P. Horowitz, H. Winfield, *The Art of Electronics*, Cambridge University Press, New York, **1995**.
- [35] The use of an electrolyte as a gate electrode and the reference electrode to establish the gate potential is called electrochemical gating. The operating principle of this technique is that the Fermi energy of the source and drain electrodes can be raised or lowered by controlling their potentials with respect to the reference electrode. For example, driving the source electrode to more positive potentials (with respect to the reference) lowers the Fermi energy and hence the energy of the electrons within the electrode. The positive charge on the source electrode is balanced by anions in the electrolyte. The presence of excess electrolyte anions, in turn, raises the orbital energy of the surface-bound redox species. Oxidation of the redox species ensues when the potential of the source electrode reaches a level positive enough to accept an electron from the redox species.
- [36] A referee has asked how we excluded interpenetration of the monolayers. Although we cannot rule out the possibility that the two opposing SAMs interpenetrate, the fact that negligible electron transfer occurs between an electrode and the redox centers on the neighboring electrode is consistent with the mechanism proposed in Figure 3.
- [37] G. P. Kittleson, H. S. White, M. S. Wrighton, *J. Am. Chem. Soc.* **1985**, *107*, 7373.
- [38] P. G. Pickup, W. Kutner, C. R. Leidner, R. W. Murray, *J. Am. Chem. Soc.* **1984**, *106*, 1991.
- [39] T. Ikeda, C. R. Leidner, R. W. Murray, *J. Am. Chem. Soc.* **1981**, *103*, 7422.
- [40] X. L. Chen, Z. Bao, J. H. Schön, A. J. Lovinger, Y.-Y. Lin, B. Crone, A. Dodabalapur, B. Batlogg, *Appl. Phys. Lett.* **2001**, *78*, 228.
- [41] B. H. Hamadani, D. Natelson, *J. Appl. Phys.* **2004**, *95*, 1227.
- [42] H. Reiss, A. Heller, *J. Phys. Chem.* **1985**, *89*, 4207.